

## Helicity Production in the Transition to Chaotic Flow Simulated by Navier-Stokes Equation

Tsutomu Sanada

*Institute of Computational Fluid Dynamics, 1-22-3 Haramachi, Meguro-ku, Tokyo 152, Japan*  
(Received 14 September 1992)

Helicity production in a homogeneous fluid is numerically demonstrated by using steady and unsteady forced Navier-Stokes equations: Even if all Fourier components of the force do not have helicity, nonlinear interactions of the zero-helicity components can generate helicity in the flow. When the Reynolds number increases, the flow nature changes from steady to temporally periodic to chaotic. The produced helicity has the largest time-averaged value in the periodic motion.

PACS numbers: 05.45.+b, 47.27.Cn, 47.52.+j

Helical motions in a flow field are considered to play an important role in the process of vortex reconnection and the generation of turbulence structures [1]. The helicity, defined as the space average of the inner product of velocity and vorticity, characterizes the helical motions. In spite of its fundamental importance, investigations about helicity have not been fruitful until recently, perhaps because a direct measurement of the instantaneous six components of velocity and vorticity is exceedingly difficult in the experimental procedures. However, the recent advent of the method of direct numerical simulation of Navier-Stokes (NS) flow has provided a new avenue to study helicity at low to moderate Reynolds numbers.

Helicity (as well as kinetic energy) is a conserved quantity in the dynamics of the three-dimensional Euler equation, and thus it is considered a fundamental quantity in the statistics of NS turbulence [2-7]. For example, besides the usual Kolmogorov energy spectrum, the universal helicity spectrum is proposed as a result of the helicity cascade theory [5-7]. It is also conjectured that alignment of velocity and vorticity induces spontaneous breaking of parity invariance of the flow and leads to the formation of highly energy-dissipating structures [4]. These conjectures are now under investigation.

In contrast to the energy, which is positive definite, helicity does not have a definite sign. Owing to this property, some interesting phenomena are observed in the generation of helicity. If a flow field is isotropic and parity invariant, the helicity is zero. However, zero helicity does not always imply the parity invariance. In other words, the condition that helicity is zero is weaker than the condition of parity invariance. For a clear understanding of this point, let us consider a flow under some forcing. Periodic boundary conditions and the initial condition of no flow ( $\mathbf{u}=0$ ) are assumed. A parity-invariant force creates a flow field with parity invariance, although an instability breaking the invariance may appear at a relatively large Reynolds number. On the other hand, a zero-helicity force does not always generate a zero-helicity flow. The generation of nonzero helicity flow by a zero-helicity forcing has already been demonstrated for the three-dimensional incompressible flow displaying the anisotropic kinetic alpha instability: Flow stirred at small

scales by an anisotropic force lacking parity invariance (but having no helicity) can generate strongly helical structures at larger scales [8-10]. Actually the helicity of the force used in Refs. [8-10] was zero for all Fourier components, although it was not explicitly mentioned in the references.

Since helicity production induced by a forcing all of whose components have zero helicity is impossible in the linear-diffusion-equation system, such production is essentially a nonlinear effect. It therefore seems to be almost impossible to analytically estimate the helicity produced in the flow. So the present paper employs a numerical approach: The production due to nonlinearity is demonstrated by means of numerical perturbation analysis of the steady NS equation and direct numerical simulation of the unsteady NS equation. Although the perturbation analysis is possible only for steady-state equations and at low Reynolds numbers, we use it to demonstrate analytically that nonlinearity causes the production of helicity. On the other hand, the unsteady NS equation can be handled numerically through the direct simulation technique, and we employ it to investigate the helicity production at relatively larger Reynolds numbers. While the main interest of Refs. [8-10] is the inverse cascade of helicity, the present paper discusses the helicity production itself. In particular, the variation of the helicity along the transition to chaotic flow is investigated.

Let us first consider the helicity production in the velocity field  $\mathbf{u}$  governed by the linearized incompressible NS (diffusion) equation:

$$\partial \mathbf{u} / \partial t = \nu \Delta \mathbf{u} + \mathbf{f}, \quad (1)$$

where  $\nu$  is the kinematic viscosity and  $\mathbf{f}$  is a forcing. We assume  $2\pi$ -space periodicity for  $\mathbf{u}$  and  $\mathbf{f}$ . Under other boundary conditions such as nonslip condition, vorticity or helicity may emerge from the boundaries. Helicity production in the boundary layer is also an important problem, but is not within the scope of our research.

In the Fourier space, Eq. (1) is written as

$$\partial \hat{\mathbf{u}}(\mathbf{k}) / \partial t = -\nu k^2 \hat{\mathbf{u}}(\mathbf{k}) + \hat{\mathbf{f}}(\mathbf{k}). \quad (2)$$

Here a caret denotes the Fourier component and  $\mathbf{k}$  is the wave vector. The relationship between the helicities of

$\hat{\mathbf{u}}(\mathbf{k})$  and  $\hat{\mathbf{f}}(\mathbf{k})$  in the steady state is obtained as

$$h[\hat{\mathbf{u}}(\mathbf{k})] \equiv i\mathbf{k} \times \hat{\mathbf{u}}(\mathbf{k}) \cdot \hat{\mathbf{u}}(-\mathbf{k}) = (\nu k^2)^{-2} h[\hat{\mathbf{f}}(\mathbf{k})]. \quad (3)$$

Here  $h[\ ]$  denotes the helicity of each Fourier component (helicity spectral density), and the total helicity is expressed by  $H_v = \langle \mathbf{u} \cdot \nabla \times \mathbf{u} \rangle = \sum_{\mathbf{k}} h[\hat{\mathbf{u}}(\mathbf{k})]$ . Equation (3) means that if the helicity of  $\hat{\mathbf{f}}(\mathbf{k})$  is zero [for example, if the three complex components of  $\hat{\mathbf{f}}(\mathbf{k})$  have the same ar-

gument] for every  $\mathbf{k}$ , then it is impossible to produce  $H_v$ .

Next consider the effect of the nonlinear term of the steady-state NS equation on helicity production. A perturbation analysis of the equation enables us to understand the effect intuitively. The equation for the present case is written as

$$\nu k^2 \hat{\mathbf{u}}(\mathbf{k}) = \hat{\mathbf{f}}(\mathbf{k}) + \mathbf{M}[\hat{\mathbf{u}}(\mathbf{p}), \hat{\mathbf{u}}(\mathbf{q}); \mathbf{k}], \quad (4)$$

where

$$\mathbf{M}[\hat{\mathbf{u}}(\mathbf{p}), \hat{\mathbf{u}}(\mathbf{q}); \mathbf{k}] = -(i/2) \sum_{\mathbf{p}+\mathbf{q}=\mathbf{k}} \{[\mathbf{k} \cdot \hat{\mathbf{u}}(\mathbf{p})]\hat{\mathbf{u}}(\mathbf{q}) - [\mathbf{k} \cdot \hat{\mathbf{u}}(\mathbf{q})]\hat{\mathbf{u}}(\mathbf{p}) - (2\mathbf{k}/k^2)[\mathbf{k} \cdot \hat{\mathbf{u}}(\mathbf{p})][\mathbf{k} \cdot \hat{\mathbf{u}}(\mathbf{q})]\}. \quad (5)$$

The second (nonlinear) term on the right-hand side of Eq. (4) is supposed to be a perturbation term. Then the zeroth- and the first-order solutions of (4), respectively, are

$$\hat{\mathbf{u}}^0(\mathbf{k}) = (\nu k^2)^{-1} \hat{\mathbf{f}}(\mathbf{k}), \quad (6)$$

$$\hat{\mathbf{u}}^1(\mathbf{k}) = (\nu k^2)^{-1} \hat{\mathbf{f}}(\mathbf{k}) + (\nu^3 k^2)^{-1} \mathbf{M}[p^{-2} \hat{\mathbf{f}}(\mathbf{p}), q^{-2} \hat{\mathbf{f}}(\mathbf{q}); \mathbf{k}]. \quad (7)$$

Further the  $(n+1)$ th-order perturbed solution is obtained from the  $n$ th order by recursion:

$$\hat{\mathbf{u}}^{n+1}(\mathbf{k}) = (\nu k^2)^{-1} \{\hat{\mathbf{f}}(\mathbf{k}) + \mathbf{M}[\hat{\mathbf{u}}^n(\mathbf{p}), \hat{\mathbf{u}}^n(\mathbf{q}); \mathbf{k}]\}. \quad (8)$$

If the amplitude of  $\hat{\mathbf{f}}(\mathbf{k})$  is small and/or  $\nu$  is large (Reynolds number is small), we expect that  $\hat{\mathbf{u}}^n(\mathbf{k})$  converges to the exact solution of Eq. (4) as  $n \rightarrow \infty$ .

If  $h[\hat{\mathbf{f}}(\mathbf{k})] = 0$ , then the helicity of  $\hat{\mathbf{u}}^0(\mathbf{k})$  is zero, but that of  $\hat{\mathbf{u}}^n(\mathbf{k})$  ( $n \geq 1$ ) may not be zero. For example, we have

$$h[\hat{\mathbf{u}}^1(\mathbf{k})] = i(\nu^4 k^4)^{-1} \{\mathbf{k} \times \hat{\mathbf{f}}(\mathbf{k}) \cdot \mathbf{M}_f(-\mathbf{k}) + \mathbf{k} \times \mathbf{M}_f(\mathbf{k}) \cdot \hat{\mathbf{f}}(-\mathbf{k})\} + i(\nu^6 k^4)^{-1} \{\mathbf{k} \times \mathbf{M}_f(\mathbf{k}) \cdot \mathbf{M}_f(-\mathbf{k})\}. \quad (9)$$

Here

$$\mathbf{M}_f(\mathbf{k}) = \mathbf{M}[p^{-2} \hat{\mathbf{f}}(\mathbf{p}), q^{-2} \hat{\mathbf{f}}(\mathbf{q}); \mathbf{k}] \quad (10)$$

is a second-order function of  $\hat{\mathbf{f}}$ , and thus Eq. (9) is the third order. Even if  $h[\hat{\mathbf{f}}(\mathbf{k})] = 0$ , the triad interaction of  $\hat{\mathbf{f}}(\mathbf{k})$  may make  $h[\hat{\mathbf{u}}^1(\mathbf{k})] \neq 0$ . From a physical point of view, it means that a zero-helicity flow is directly induced by the zero-helicity forcing, and it is deformed by the nonlinear effect. The deformation, which remains under the forcing, can produce helicity in the flow.

This perturbation procedure is numerically executed for the confirmation of the helicity production. Equation (8) along with (6) gives recursively higher-order perturbed solutions. We have used the wave number space of  $-10 \leq k_1, k_2, k_3 \leq 10$  for  $\hat{\mathbf{u}}(\mathbf{k})$ , but the forcing is limited only to  $-2 \leq k_1, k_2, k_3 \leq 2$ . The forcing is steady

and  $h[\hat{\mathbf{f}}(\mathbf{k})] = 0$  for every  $\mathbf{k}$ . Random numbers are used for assigning the amplitudes and phases to  $\hat{\mathbf{f}}(\mathbf{k})$ . The characteristic length and time of  $\mathbf{f}$  are estimated, respectively, as  $L = (\langle \mathbf{f}^2 \rangle / \langle (\nabla \times \mathbf{f})^2 \rangle)^{1/2} = 0.69$  and  $T = (\langle (\nabla \times \mathbf{f})^2 \rangle)^{-1/4} = 2.5$ , and are used for the normalizations of time, energy, enstrophy, and helicity. Also the Reynolds number is defined as  $\text{Re} = L^2 T^{-1} / \nu = 0.19 / \nu$ .

Figure 1 shows the relationship between the perturbation order  $n$  and the (total) helicity produced in the corresponding perturbed field for different values of  $\nu$  ( $=0.1, 0.09$ , and  $0.08$ , respectively, corresponding to  $\text{Re} = 1.9, 2.1$ , and  $2.4$ ). For all the values of  $\nu$  considered here, helicity becomes negative for  $n=1$ , but then goes through oscillatory transients, and finally converges to positive asymptotic (steady) values for  $n \gtrsim 10$ . Because of the oscillatory behavior of helicity for relatively small  $n$ , a low-

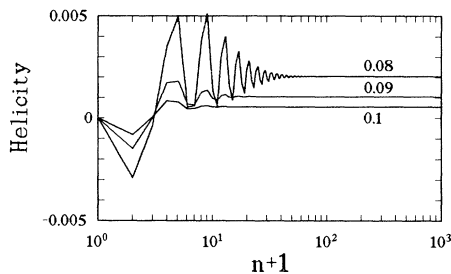


FIG. 1. Helicity production as a function of the order  $n$  of perturbation analysis for  $\nu = 0.1, 0.09$ , and  $0.08$ .

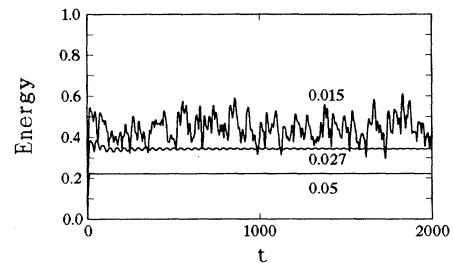


FIG. 2. Time evolution of energy for  $\nu = 0.05, 0.027$ , and  $0.015$ .

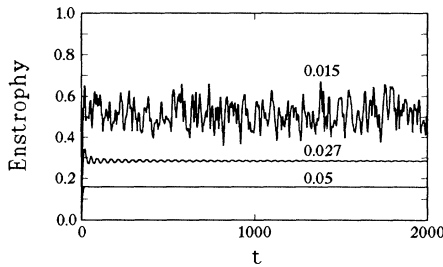


FIG. 3. Time evolution of enstrophy for  $\nu=0.05, 0.027,$  and  $0.015$ .

order perturbation may not be sufficient for a proper estimation of the steady-state value of helicity. The converged value increases with decreasing of  $\nu$ ; the produced helicity increases as the nonlinearity becomes stronger. The case of  $\nu=0.08$  takes much longer to converge and it may be close to the convergence limit of the perturbation series. [Here we should note that the limit depends also on the amplitude of  $\mathbf{f}(\mathbf{k})$ . Under a sufficiently small amplitude, the series converges even if  $(\nu k^2)^{-1} \gtrsim 1$  for some  $\mathbf{k}$ .] It has been observed that for  $\nu=0.075$  some oscillation appears even at  $n=1000$ , and it does not appear to damp out completely. When  $\nu$  is further reduced to a value of  $0.07$ , calculations beyond about  $n=25$  are impossible owing to numerical overflows. Values of  $\nu$  smaller than that used in the perturbation analysis are investigated later by directly simulating the unsteady NS equation.

Before presenting the simulation results, we consider the dynamics of helicity by using the incompressible NS equation:

$$\partial \mathbf{u} / \partial t + (\mathbf{u} \cdot \nabla) \mathbf{u} = -\nabla p + \nu \Delta \mathbf{u} + \mathbf{f}, \quad (11)$$

$$\nabla \cdot \mathbf{u} = 0. \quad (12)$$

The time-evolution equation of helicity  $H_v$  is obtained as

$$dH_v / dt = 2\langle \boldsymbol{\omega} \cdot \mathbf{f} \rangle - 2\nu H_\omega. \quad (13)$$

Here  $H_\omega = \langle \boldsymbol{\omega} \cdot \nabla \times \boldsymbol{\omega} \rangle$  is helicity of vorticity ( $\boldsymbol{\omega} = \nabla \times \mathbf{u}$ ), which does not have a definite sign, just like  $H_v$ . Negative  $H_\omega$  increases  $H_v$ , while positive  $H_\omega$  decreases it. The

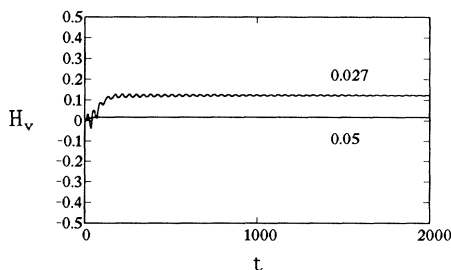


FIG. 4. Time evolution of helicity  $H_v = \langle \mathbf{u} \cdot \nabla \times \mathbf{u} \rangle$  for  $\nu=0.05$  and  $0.027$ .

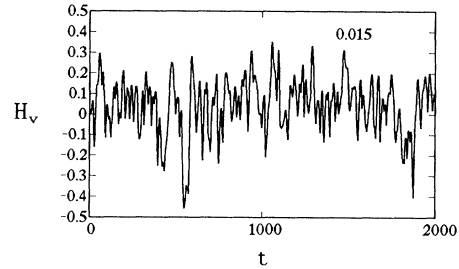


FIG. 5. Time evolution of helicity for  $\nu=0.015$ .

correlation between the signs of  $H_v$  and  $H_\omega$  is therefore an important factor in the evolution of helicity. We obtain through a simple calculation

$$-\langle \mathbf{u} \cdot \Delta \mathbf{u} \rangle = \langle \mathbf{u} \cdot \nabla \times \nabla \times \mathbf{u} \rangle = \langle \nabla \times \mathbf{u} \cdot \nabla \times \mathbf{u} \rangle > 0. \quad (14)$$

This means that  $\mathbf{u}$  and  $-\Delta \mathbf{u}$  have more of a tendency to be parallel than to be antiparallel. Thus  $\langle \mathbf{u} \cdot \nabla \times \mathbf{u} \rangle = H_v$  and  $-\langle \Delta \mathbf{u} \cdot \nabla \times \mathbf{u} \rangle$  probably have the same sign. Noting  $-\langle \Delta \mathbf{u} \cdot \nabla \times \mathbf{u} \rangle = \langle \boldsymbol{\omega} \cdot \nabla \times \boldsymbol{\omega} \rangle = H_\omega$ , we conjecture that  $H_v$  and  $H_\omega$  have the same sign. If this conjecture is correct, the term  $-2\nu H_\omega$  in Eq. (13) reduces the magnitude of  $H_v$ , regardless of its sign, and hence behaves like a viscous dissipation for helicity. This will be confirmed in the following simulation result.

A direct simulation of the unsteady NS equation demonstrates the helicity production at a  $Re$  larger than that in the perturbation analysis. The simulation is done by the spectral method in the same truncated Fourier space and with the same forcing as in the perturbation analysis. The time advancement from the initial condition of  $\mathbf{u}=0$  is by second-order Runge-Kutta scheme. When  $\nu=0$  and  $\mathbf{f}=0$ ,  $H_v$  should be a conserved quantity [see Eq. (13)]. The spectral method is quite suitable for maintaining this property. For  $\nu=0.1, 0.09,$  and  $0.08$ , the direct simulation gives the steady solutions in good agreement with those obtained by the perturbation analysis. Further we are also able to employ several smaller values of  $\nu$  ( $0.01 < \nu < 0.08$ ).

It is possible to divide the values of  $\nu$  into the following three ranges, in relation to the time evolutions of energy and enstrophy:  $0.03 < \nu < 0.08$  ( $6.3 > Re > 2.4$ )—steady

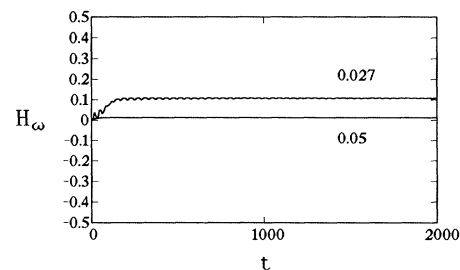


FIG. 6. Time evolution of helicity of vorticity  $H_\omega = \langle \boldsymbol{\omega} \cdot \nabla \times \boldsymbol{\omega} \rangle$  for  $\nu=0.05$  and  $0.027$ .

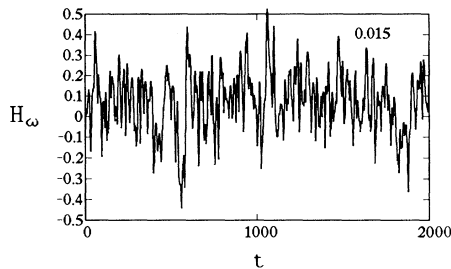


FIG. 7. Time evolution of helicity of vorticity for  $\nu=0.015$ .

motion,  $0.022 < \nu < 0.027$  ( $8.6 > \text{Re} > 7.0$ )—periodic motion, and  $0.01 < \nu < 0.02$  ( $19 > \text{Re} > 9.5$ )—chaotic evolution. Representative evolutions of energy and enstrophy are shown, respectively, in Figs. 2 and 3, which indicate steady, periodic, and chaotic evolutions. Even for the largest  $\text{Re}$  flow, the inner wave number space  $-5 \leq k_1, k_2, k_3 \leq 5$  contains more than 99% of the total energy in the full space  $-10 \leq k_1, k_2, k_3 \leq 10$ . We can therefore say that the number of Fourier modes is sufficient to simulate these flows.

Figures 4–7 show the evolutions of  $H_v$  and  $H_\omega$ . These figures also exhibit steady, periodic, and chaotic motions, respectively, for  $\nu=0.05$ , 0.027, and 0.015. As conjectured before, the signs of  $H_v$  and  $H_\omega$  in the steady and periodic motions are the same except for the initial transition phase. In the chaotic motion,  $H_v$  and  $H_\omega$  vary irregularly with time, but the signs of  $H_v$  and  $H_\omega$  are the same for about 85% of the period  $0 < t < 2000$ . The previous conjecture about the signs of  $H_v$  and  $H_\omega$  seems to be acceptable also in this chaotic motion.

Energy, enstrophy, and helicity against  $\text{Re}$  are shown in Fig. 8, in which for periodic (the range “P”) and chaotic (the range “C”) motions, values obtained by time average over  $400 < t < 2000$  are used. Energy and enstrophy display a rather slow monotonic increase with  $\text{Re}$  in the entire range. On the other hand, helicity increases very rapidly in the range “S,” reaches a maximum somewhere inside “P,” and starts displaying an oscillatory behavior in the range “C.” In the transition from periodic to chaotic, the nonlinearity becomes stronger (because  $\text{Re}$  increases), but it produces only *less* helicity.

In summary, helicity can be produced by a forcing whose helicity spectral density is zero, due to the non-

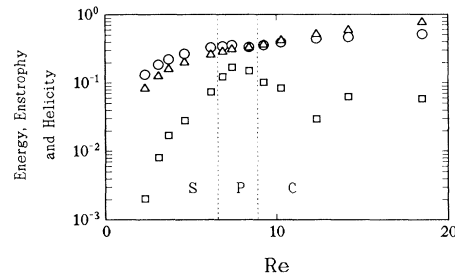


FIG. 8. Energy ( $\circ$ ), enstrophy ( $\Delta$ ), and helicity ( $\square$ ) as a function of Reynolds number. “S” means the range of steady motion, “P” is for the periodic, and “C” is for the chaotic.

linear effect of the NS equation. Such a helicity production has been demonstrated numerically by the perturbation analysis and the direct simulation of the NS equation. In the steady and the periodic motions, the helicity increases with  $\text{Re}$ . However, when the motion becomes chaotic, the time-averaged value of the helicity goes down. There seems to be a strong relationship between the production-reduction of helicity and the transition to chaos, indicating that helicity dynamics may play a key role in the onset of unstable flow.

The author is grateful to B. Galanti, K. Ishii, K. Kuwahara, and V. Shanmugasundaram for useful discussions and encouragement.

- [1] See, for example, *Topological Fluid Mechanics*, edited by H. K. Moffat and A. Tsinober (Cambridge Univ. Press, Cambridge, 1989).
- [2] E. Levich and A. Tsinober, *Phys. Lett.* **93A**, 293 (1983).
- [3] A. Tsinober and E. Levich, *Phys. Lett.* **99A**, 321 (1983).
- [4] E. Levich and L. Shtilman, *Phys. Lett. A* **126**, 243 (1988).
- [5] W. Polifke and L. Shtilman, *Phys. Fluids A* **1**, 2025 (1989).
- [6] W. Polifke, *Phys. Fluids A* **3**, 115 (1991).
- [7] A. V. Tur and E. Levich, *Fluid Dyn. Res.* **10**, 75 (1992).
- [8] U. Frisch, Z. S. She, and P. L. Sulem, *Physica (Amsterdam)* **28D**, 382 (1987).
- [9] P. L. Sulem, Z. S. She, H. Scholl, and U. Frisch, *J. Fluid Mech.* **205**, 341 (1989).
- [10] B. Galanti and P. L. Sulem, *Phys. Fluids A* **3**, 1778 (1991).